Investigation of the potential of thermophotovoltaic heat recovery for the Turkish industrial sector

CrossMark

Zafer Utlu [a,*], Ufuk Parali [b]

[a] İstanbul Aydin University, Engineering and Architecture Faculty, Mechanical Engineering Department, Florya, TR 34455 Istanbul, Turkey
[b] İstanbul Aydin University, Engineering and Architecture Faculty, Electrical and Electronics Engineering Department, Florya, TR 34 455 Istanbul, Turkey

ABSTRACT

Thermophotovoltaics (TPV) are the use of the photovoltaic effect to generate electricity from a high-temperature thermal (infrared) source. This study deals with to provide an overview of heat recovery by TPV from industrial high-temperature processes in Turkish industrial sector. The paper reviews the relevant facts about TPV technology and the high-temperature industry and identifies three principle locations for TPV heat recovery. For each location, one example process is assessed in terms of applicability of TPV impact on the existing process and power scale. Knowledge of these factors should contribute to the design of an optimum TPV system. In the TIS, the total technical–potential energy recovery in the high-temperature industry using deployed and demonstrated heat recovery devices for product, flue gas, and wall heat recovery was estimated as 447.8 PJ/year. However, an estimation from 22.40 PJ/year to 67.45 PJ/year can be achieved according to the TPV efficiencies. Also, the paper estimates the range of possible energy savings and the reduction in CO emission using TPV in the high-temperature industry. It is expected that this study will be very beneficial in developing energy policies of countries in terms of the usage of waste energy efficiency.

1. Introduction

Owing to the high prices of energy and decreasing fossil fuel resources, the optimum application of energy and the energy consumption management methods and waste management and heat recovery methods for reuse of waste heat have become very important. In a modern industrial society, the majority of energy is consumed in the sectors of industry transportation and residential–commercial where fossil fuels being the primary sources of this energy. The use of fossil fuels has led to worldwide concerns about security of supply increasing energy demand limitation of resources and local and global environment impacts (e.g., acid rain, climate change). A consequence is increased interest in non-fossil fuel energy resources and the efficient use of fuel.

Industrial sector accounts for about two–fifth of total final energy use in most countries. Energy consumption in the industrial sector depends mainly on the available amounts of local resources which are closely connected with the present rural economy and industrializing. Fig. 1 illustrates energy flows in a macro system for the industrial sector including energy carriers and its subsectors [1].

The energy balance is the basic method of process investigation. It makes the energy analysis possible by clarifying the key points of the needs for the improvement and the optimization of the process, and it is the key to optimization. Energy efficiency can be measured by economic or physical indicators. The manufacturing industry, and especially the energy-intensive (or low, medium, and high temperatures) industry, commonly applies the Specific Energy Consumption (SEC) as a physical indicator [1]. The SEC is defined as the energy requirement per output of the process (e.g., GJ/tonne). Reduction in the SEC for the manufacturing industry can be achieved by various measures such as process optimization, improved or modified combustion, energy management of Combined Heat and Power (CHP), improved insulation and heat recovery.

The capital and operation cost of the measure can be compared with reduced energy costs (achieved through reduced SEC) and both costs will decisively determine the payback period. Several combustion-based Thermophotovoltaic (TPV) systems mainly for CHP or portable power applications are in a prototype stage. It is mentioned here that the industry has a large demand for steam and hot water. It used as 1038 PJ/year in 2010 in the Turkish Industrial Sector (TIS) [1] which was a large potential CHP market for TPV. This paper considers TPV as a heat recovery method that generates electricity from available high-temperature processes in the TIS industry. The method has been suggested in previous publications [2–9], and NPAC has examined heat recovery by TPV specifically for the glass industry [7].

* Corresponding author. Tel.: +90 532 554 78 27; fax: +90 212 388 85 62.
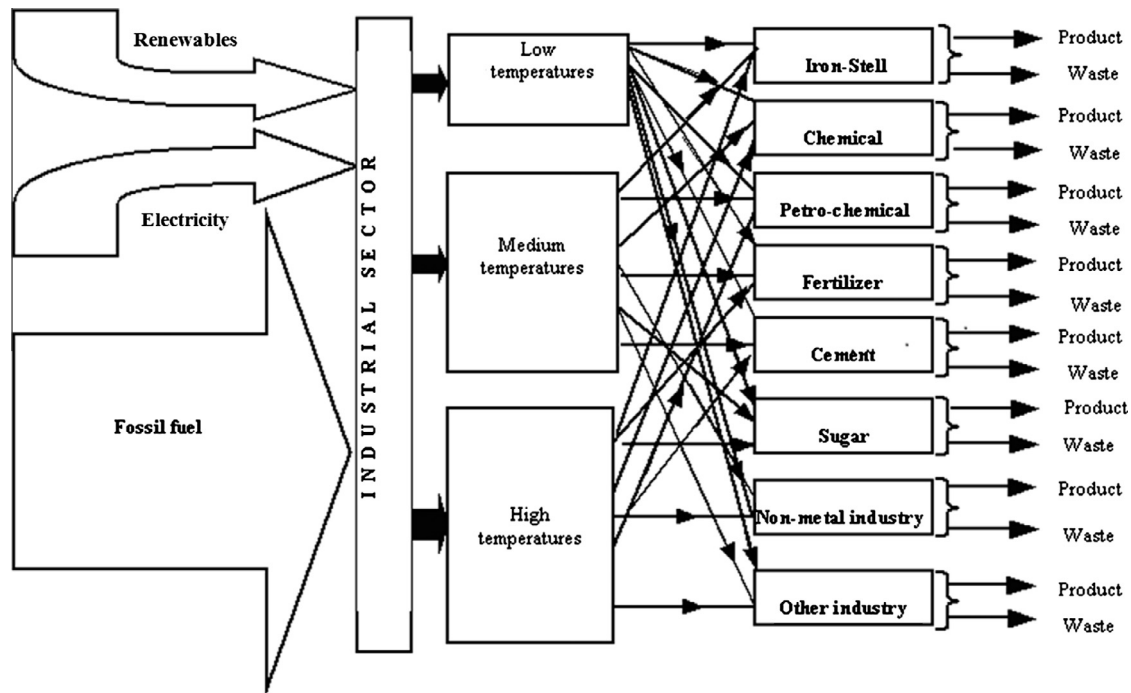E-mail addresses: zaferutlu@aydin.edu.tr, zafer_utlu@yahoo.com (Z. Utlu).

Fig. 1. An illustrative presentation of the energy flows in an industrial sector for countries.

Other technologies are mostly in the research and development stage operating in different temperature ranges, including the following [2,9–13];

· *Low temperature*: Turbine using organic rankine cycle with a generator. Thermoelectric systems (Seebeck, thermocouple effect).
· *Medium temperature*: Stirling engine with a generator. Direct use of flue gas with a turbine and a generator, metal hydride systems, zeolite systems, and active magnetic regenerator systems.
· *High temperature*: Thermophotovoltaic systems.

The primary objective of the present study is to investigate the potential of thermophotovoltaic heat recovery for the Turkish Industrial Sector by presenting a case study based on the actual data. In this regard, construction of thermophotovoltaics is given first. Next, TIS and its subsectors such as iron–steel, chemical–petrochemical, petrochemical–feedstock, cement, fertilizer, sugar, non-iron metal industry, and other industries are investigated in terms of heat recovery. Then, the potential of thermophotovoltaic heat recovery for the TIS is determined. Finally, three principle locations for the available TPV technology are identified as follows: product, flue gas, and wall heat recovery, and for each location, one example process is assessed in more detail, and the results obtained are discussed.

2. Technology of thermophotovoltaic

The investigations in the field of TPV converters started in the early 1960s. However, the real advantage of the TPV systems has been shown only in the past two decades [14]. TPV technology is one of the possible choices in the development of a small device for producing on-site electricity [15–19]. Portability and the relatively small dimensions of these devices make them advantageous to use not only in the various industries but also for everyday applications where power generation for buildings, hospitals, offices, and electric vehicles are a few examples [20]. They

can be utilized and fit easily into various places for capturing waste heat from variety of sources and store that energy in a battery or device where it can be available for future use [15–17]. The main use of a TPV generator can be in the distributed combined heat and power generation [21]. The TPV systems have been proposed for portable generators [21–23], cogeneration systems [21,24], combined cycle power plants, and solar power plants [21,25]. In addition to these, the usage of TPV systems in the automotive sector especially for the hybrid vehicles and in the high-temperature industries such as glass, steel-iron, and petrochemical has also been analyzed in the literature [21,26,27]. Further studies were developed in military and space sectors [28]. The usage of TPV systems provides the following advantages: high fuel utilization factor and low noise level since there is no moving part on a TPV and easy maintenance [21,29]. They have also great fuel flexibility since the radiator of a TPV system, generally made by refracting materials such as tungsten or ceramic oxides, may be heated by various fuel typologies such as fossil fuels (natural gas, oil, coke, etc.), municipal solid wastes, and nuclear fuels or by highly concentrated solar radiation [14,19–21,30–34]. It is also possible to couple them with combustion devices such as domestic boilers. In addition to these, a TPV system usually allows very low pollutant emissions [21].

TPV systems are static energy converters [35]. They convert the infrared blackbody radiation (thermal energy) into electricity. They work in the same way that photovoltaic (PV) devices convert visible light (solar energy) into electricity [21,32,36–38]. In contrast to solar PVs, TPV systems can achieve higher efficiency and higher output power density, because of the lower band gap and the closer distance between the emitter and the active region of the TPV diode [35]. The typical TPV device consists of four main parts. These are emitter-heated by a thermal energy source, radiator or filter for spectral control, collector (PV diode), and reflector, as can be seen in Fig. 2 [15,17]. TPV system allows to utilize the selective emitter (for example, made of tungsten) and selective filters/mirrors, back surface reflectors for sub-band gap photon reflection to the emitter which ensures efficiency increase owing to better matching in the radiation and PV cell photosensitivity spectra
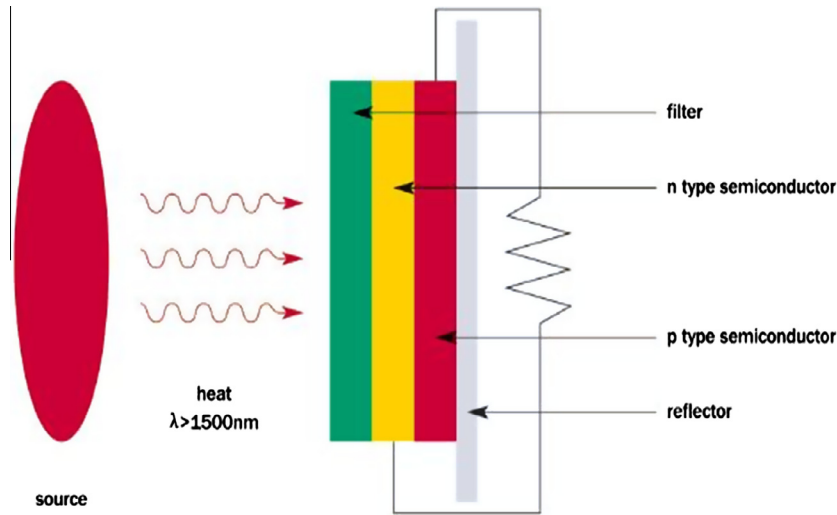
Fig. 2. Schematic drawing of a basic TPV cell [15].

[30]. Combining a selective emitter with a back surface reflector on a PV cell is a method of spectral control that provides higher overall TPV efficiency, which is strongly dependent upon the quality of the spectral control [39]. Without spectral control, TPV energy conversion suffers dramatically [37]. Another parameter of the emitter of the PV cell for efficiency is its distance from the TPV diode. In the far field TPV, radiation heat transfer is limited by the density of states in vacuum to σT^4 where σ is the Stefan–Boltzmann constant and T is the temperature in Kelvin. However, for a TPV with a microscale-gap between the emitter and the TPV diode, the small submicron gap enables energy within the hot radiator to evanescently couple or tunnel directly to the TPV diode, resulting in a higher limit of $n^2\sigma T^4$ for dielectrics of index n [40]. Thus, radiation heat transfer from the hot radiator to the TPV diode can be increased significantly (see Fig. 3), resulting in the potential for large gains in electrical output power density [40–42].

As mentioned above, TPV systems that are solid-state devices convert heat into electricity. This is done by converting photons due to thermal radiation into electron–hole pairs via a low band gap PV medium, and these electron–hole pairs produce current [19–21,34]. The device converts secondary thermal radiation, re-emitted by an absorber or heat source into electricity, where the 550 °C to over 800 °C temperatures can generate enough waste heat to recycle using TPV technology. Currently, TPV diodes are more sensitive to infrared radiation ($\lambda > 1500$ nm) from surfaces that are at temperatures from 950 °C to about 1350 °C [15,17]. TPV devices are based on diodes, with band gaps lower than 0.75 eV, which can contain a single type of semiconductor or several different types to cover a broad range of temperatures, and are designed for maximum efficiency at the wavelength of the secondary radiation. Therefore, most of the TPV research has concentrated on semiconductors such as gallium antimonide, GaSb, indium gallium arsenide, InGaAs, indium gallium arsenic antimonide, InGaAsSb, and indium arsenic antimony phosphide, InAsSbP, which are all direct band gap semiconductors [34,39]. On the other hand, despite their great promise, small experimental TPV systems at 1000 K generally exhibit low power conversion efficiencies (approximately 1%), due to heat losses such as thermal emission of undesirable mid-wavelength infrared radiation [19]. In order to overcome this problem, it is shown in the literature that photonic crystals (PhCs) have the potential to strongly suppress such losses [19].

The efficiency discussion of a TPV generator can be done either in the means of PV cell efficiency [36], η_{TPV}, or in the means of TPV system (see Fig. 4 for the schematic of a generic TPV system) efficiency, $\eta_{EL,TPV}$, which also covers the PV cell power conversion efficiency [21]. For the discussion of PV cell efficiency, we can define η_{TPV} as follows:

$$\eta_{TPV} = \eta_{Spectral} \times \eta_{PV} \tag{1}$$

where $\eta_{Spectral}$ is the spectral efficiency and η_{PV} is the photovoltaic (PV) cell efficiency [21,36]. Spectral efficiency can be defined as the ratio between the whole radiation from the emitter and the part of the radiation that passes through the filter which is resembled as $P'_{spectral}$. Filter is utilized in order to match the spectral emission of the emitter to PV cell. Thus, we can define spectral efficiency as follows [21]:

$$\eta_{Spectral} = P'_{spectral}/P_{Rad} \tag{2}$$

where P_{Rad} is the radiant power from the emitter calculated according to the Stefan–Boltzmann's law:

$$P_{Rad} = \in \cdot S_{em} \cdot 2\pi \int_0^\infty I(\lambda; T_{em})d\lambda =$$
$$\in \cdot S_{em} \int_0^\infty \frac{2\pi hc^2}{\lambda^5}\left[exp\left(\frac{hc}{\lambda k_B T_{em}}\right) - 1\right]^{-1}d\lambda \tag{3}$$

where $k_B = 1.380 \times 10^{-23}$ J K^{-1} and $h = 6.626 \times 10^{-34}$ J s are the Boltzman and Plank constant, respectively, $c = 2.99 \times 10^8$ m s^{-1} is the speed of light, λ is the wavelength, ε is the emissivity of the body, S_{em} is the area of the emitter surface, T_{em} is the emitter temperature, and $I(\lambda; T_{em})$ is the radiant intensity [21,43,45]. $P'_{Spectral}$ can be estimated by integrating the radiant intensity in the range of wavelengths (from 0 to λ_{gap}) which passes through the filter:

$$P'_{Spectral} = \in \cdot S_{em} \int_0^{\lambda_{gap}} I(\lambda; T_{em})\tau(\lambda)d\lambda =$$
$$\in \cdot S_{em} \int_0^{\lambda_{gap}} \frac{2\pi hc^2}{\lambda^5}\left[exp\left(\frac{hc}{\lambda k_B T_{em}}\right) - 1\right]^{-1}\tau(\lambda)d\lambda \tag{4}$$

where $\tau(\lambda)$ resembles the transmission coefficient as a function of input radiation wavelength [21,43,44].

In the conversion of the radiant energy with TPV diodes, only a fraction of the total radiant energy is used [37]. In most of the systems, the vast majority of the emitted thermal photons have energies below the electronic band gap of the TPV cell. These photons, which are still absorbed as waste heat, do not generate electron–hole pairs and they tend to reduce TPV diode efficiency [19,36,45].
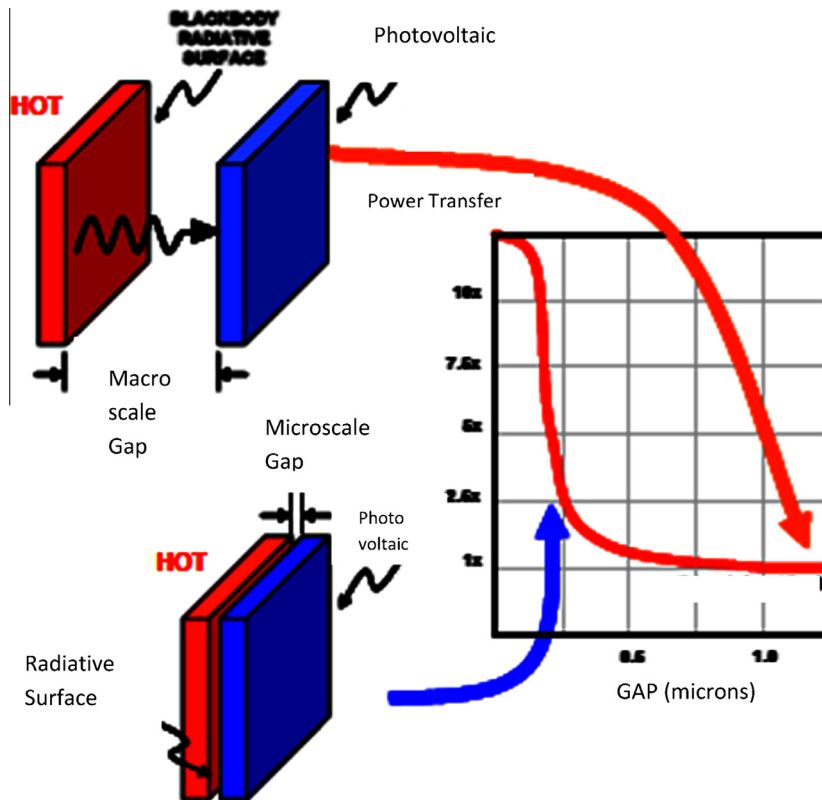
Fig. 3. Potential for large gains in power density from close spacing [40].
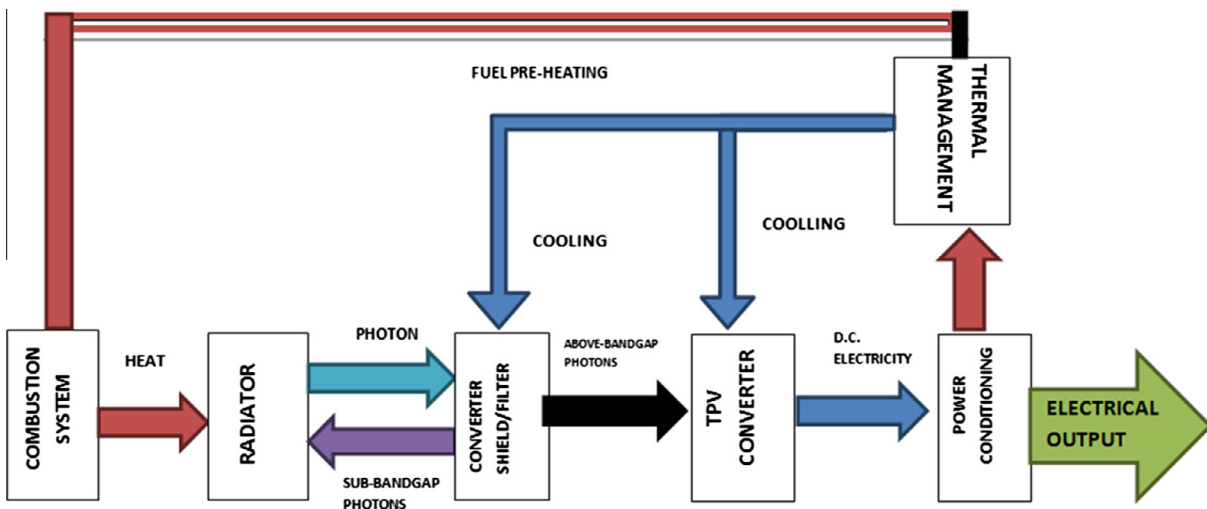

Fig. 4. Schematic of a generic TPV system.

For example, only about 26% of the radiant energy can be converted to electricity for a 950 °C radiator temperature and a 0.52 eV band gap TPV diode where the remaining 74% of the radiant energy cannot be converted to electricity since they do not generate electron–hole pairs and will be lost if absorbed [36,37,45]. Ideally, this useless energy should be reflected back to the radiator (recuperated) in order to maximize TPV efficiency [37]. Thus, spectral control is vital for a successful energy conversion in TPV systems. It is for this reason that the filter should ideally be able to block all the photons with energy lower than the PV cell band gap and pass the photons with higher energy [8,21,26]. An example of a front surface, tandem filter consisting of an edge pass filter (short pass) in series with a highly doped,

epitaxially grown layer is shown in Fig. 5 [37,46–49]. For the edge pass filter, Sb_2Se_3 ($n \sim 3.4$) is used as the high index of refraction material and YF_3 ($n \sim 1.5$) is used as the low index of refraction material [37]. These filters reflect the unusable photons which do not generate electron–hole pairs due to their smaller energies than the TPV diode band gap and let the majority of the useable photons with energies greater than the band gap pass [37]. This provides the spectral distribution of photons transmitted through the tandem filter to the TPV diode to be shifted toward the photons that can generate electricity regarding to the spectral distribution provided by an emitting surface [21,34,37,39]. Many types of filters have been developed such as plasma filters, 1-D photonic band gap filters,
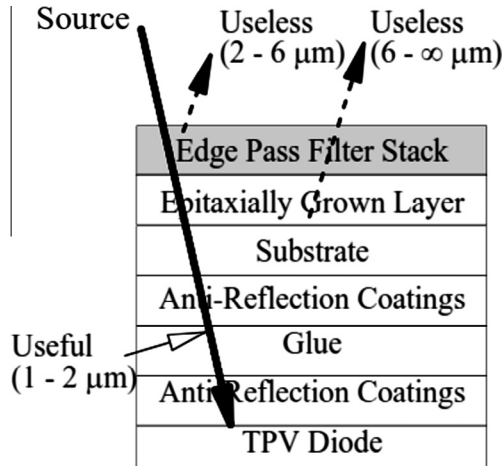
Fig. 5. Front surface tandem filter consisting of an edge pass filter in series with a highly doped epitaxially grown layer [37].

2-D photonic band gap filters, 3-D photonic band gap filters, combination of plasma filter and 1-D photonic band gap filter, dielectric stacks, or back surface reflectors [17,21,50–54]. Photon recycling via reflection of low-energy photons with a 1-D, 2-D, or 3-D reflector is a concept that significantly reduces radiative heat transfer [19,53]. This approach can also be extended to encompass the more general concept of spectral shaping: directly suppressing emission of undesirable (below band gap) photons as well as enhancing emission of desirable (above band gap) photons [19,39]. Such control is provided by complex 1-D, 2-D, and 3-D periodic dielectric structures, generally known as photonic crystals (PhCs) [19,55]. Spectral shaping has been proposed and predicted to be an effective approach for high efficiency TPV power generation [19,34,39,56–59]. This approach is illustrated in Fig. 6a and b.

The second term on the right-hand side of Eq. (1), PV cell efficiency (η_{PV}), represents the ratio between the maximum electrical power output and the incident power on the TPV cell [21,34,39,43,44,59]:
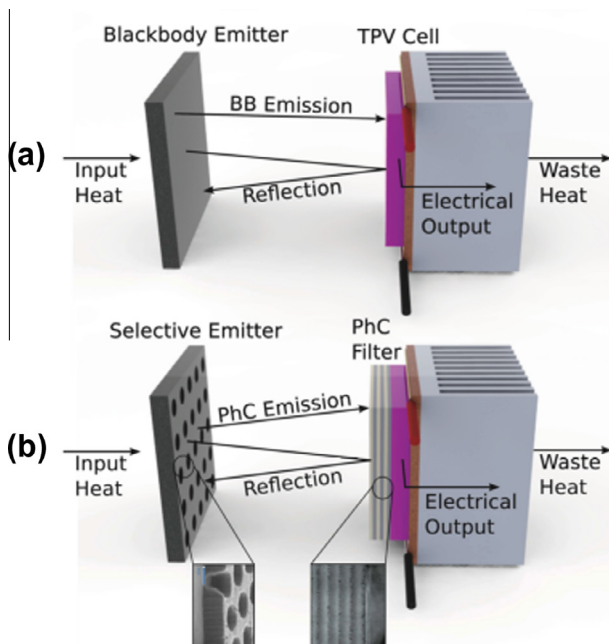

Fig. 6. (a and b) Spectral shaping approach with photonic crystals [19].

$$\eta_{PV} = \frac{P_{el.dc}}{P_{Inc.}} = \frac{V_{OC} \cdot J_{SC} \cdot FF}{P_{Inc.}} \qquad (5)$$

where V_{OC} is the open voltage circuit, J_{SC} is the short-circuit current, FF is the fill factor, and P_{inc} is the incident power on the cell (total heat absorbed in the active region of the PV cell that can be converted to electricity [36]). Finally, embedding the Eqs. (2)–(5) into Eq. (1), we can define the overall expression for TPV thermal-to-electric power conversion efficiency, η_{TPV}, as follows:

$$\eta_{TPV} = \frac{V_{OC} \cdot J_{SC} \cdot FF}{\in \cdot S_{em} \int_0^\infty \frac{2\pi E^3}{h^3 c^2 (e^{E/kT_{rad}} - 1)} dE} \qquad (6)$$

where E is the photon energy and T_{rad} is the hot side temperature of the radiator [36,39,44]. In Eq. (6), the actual value of the J_{SC} produced can be calculated as [21,60,61]:

$$J_{SC} = e \int_0^{\lambda_{GAP}} \phi(\lambda) \cdot \eta_{QE}(\lambda) d\lambda \qquad (7)$$

where e is the electron charge, $\phi(\lambda)$ is the incident photon flux, and $\eta_{QE}(\lambda)$ is the external quantum efficiency, which is one of the fundamental parameters used to estimate the conversion efficiency of a PV cell [21,34,37,43,44,59,62]. The performance of a TPV system can be evaluated through two efficiencies: the conversion efficiency and the quantum efficiency. The conversion efficiency is the ratio of the electric power generated from a TPV cell to the absorbed radiative power [29,34,37,43,44,59]. The quantum efficiency is the ratio of the number of generated electron–hole pairs that can be used for photocurrent generation to the number of photons absorbed. The quantum efficiency can be defined as a function of wavelength. It is also possible to define it as a function of energy. The quantum efficiency for a certain wavelength becomes unity if all the incident photons with that particular wavelength are absorbed and the generated minority carriers due to these photons are collected. The quantum efficiency becomes zero for the incident photons having energy below the band gap of the TPV diode [34,37,43,44,59,63]. There are two types of quantum efficiencies considered: external quantum efficiency, $\eta_{QE}(\lambda)$, and internal quantum efficiency, $\eta_{QI}(\lambda)$. The definition of the external quantum efficiency can be given as the probability that a photon of the wavelength λ is absorbed by the TPV diode, generating an electron that will be collected at the terminals [34,39,43,44]. Since it is based upon the photon flux that is incident on the semiconductor [39] and takes into consideration of the reflection and absorption of incident photons and the generation/collection of minority carriers, the behavior of the p–n junction is described by the external quantum efficiency expression in great detail [21,34,39,43,44,59–61]:

$$\eta_{QE}(\lambda) = (1 - R_i)\eta_{QI}(\lambda) \qquad (8)$$

where R_i is the reflection coefficient, $R_i = R_n$ if photons are incident on the n side of the p–n junction, and $R_i = R_p$ if photons are incident on the p side of the p–n junction. Fig. 7 shows the measured external quantum efficiencies for different semiconductors used for TPV diodes [21,60,61]. It is seen in Fig. 7 that the most of the materials used for the TPV diodes have higher external quantum efficiency than the PV diodes. This provides a particular characteristic for TPV cells and letting them reach higher conversion efficiency than PV cells [21]. The internal quantum efficiency, $\eta_{QI}(\lambda)$ seen in Eq. (8), refers to the efficiency with which light not transmitted through or reflected away from the cell can generate charge carriers that can generate current [34,39,64]. In other words, $\eta_{QI}(\lambda)$ is based upon the photon flux that enters the semiconductor [39]:

$$\eta_{QI}(\lambda) = \frac{J'_{ph}}{J_F} \qquad (9)$$

where J'_{ph} is the photon produced current density per wavelength and J_F is the maximum possible current density that can be
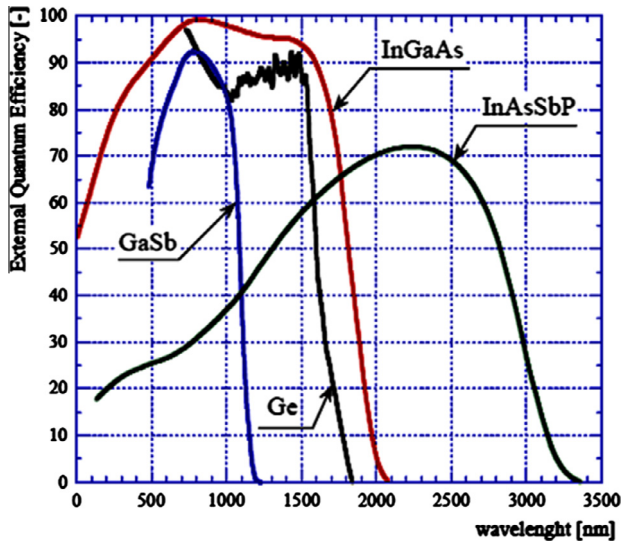
Fig. 7. Measured external quantum efficiencies for some semiconductors [21,60,61].

produced by the incident photon flux [39,59]. Therefore, internal quantum efficiency can be defined as follows:

$$\eta_{QI}(\lambda) = \bar{J}'_{qn} + \bar{J}'_{qp} + \bar{J}'_d \tag{10}$$

where J'_{qn}, J'_{qp}, and J'_d are the dimensionless photon produced current densities per wavelength in the p region, n region, and the depletion region of the p–n junction, respectively [39]. Fig. 8 shows the contribution of the current densities mentioned above to the internal quantum efficiency of p–n junction illuminated. However, in addition to the discussion above, to determine the performance of a PV cell, the non-equilibrium situation must also be considered that occurs with the recombination of the generated electron–hole pairs by the incident radiation [34,39]. Fig. 9 shows the effect of the recombination on the internal quantum efficiency, and Fig. 10 shows the schematic of a near field TPV system where the recombination and photogeneration of electron–hole pairs are depicted as
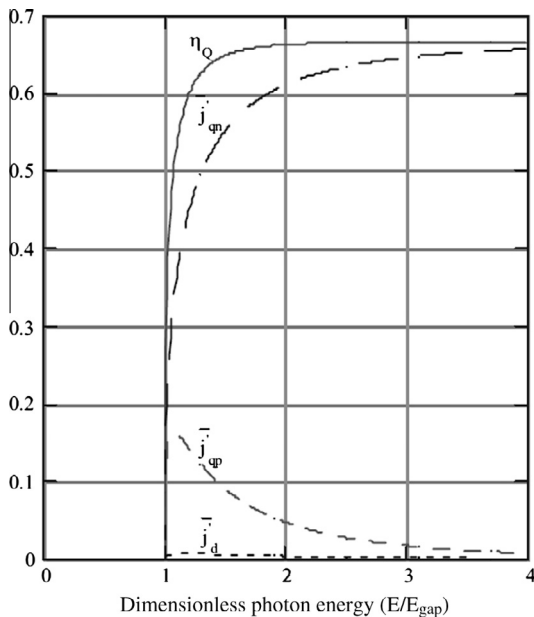
solid-state model. The minority carrier diffusion lengths and the depletion region in the p–n junction are also illustrated where In_{018}-$Ga_{0.82}Sb$ is used as the TPV cell material and a plain tungsten is used as the emitter.

Converters for TPV systems, as mentioned previously, are very similar to standard solar cells such as Si and high efficiency GaAs, but they are made of semiconductor materials with lower band gap, for better spectral matching with the emitter radiation [21,34,39]. Fig. 11 shows the relationship between the semiconductor lattice constant and the energy gap [21]. In order to match the radiation emitted by a 1000–1600 °C blackbody, few materials and alloys can be adopted, such as Ge, GaSb, InGaAs/GaSb, InGaSb/InP, and the quaternary InGaAsSb/GaSb and InGaAsP/InP [21,36,66–69].

As mentioned up to now, the heart of a TPV cell is a standard p–n (or n–p) junction made of one of the semiconductor materials listed above [21]. There are two basic techniques to realize p–n junctions for TPV: diffusion and epitaxy [21]. Diffusion of a doping element in a semiconductor usually follows Fick's law [21,70], and it only depends on the diffusion coefficients of the selected atoms in a particular material, on their concentration, and on their process temperature [21]. Fig. 12 shows GaSb and Ge cells realized by diffusion where they have the advantage of lower cost, since the process is relatively simple [34]. A better control of the emitter doping concentration and profile can be obtained by using the epitaxial technique. Ternary and quaternary cells such as InGaAs, InGaSb, InGaAsSb, and InGaAsP are realized only by epitaxy, because the alloys need a careful control of the composition [21]. Fig. 13 shows the architecture of a typical InGaAsSb n–p junction diode [36]. In the past, only single junction devices were developed for TPV applications: multi-junction designs such as amorphous-Si/crystalline-Si or InGaP/GaAs/Ge were only developed for high efficiency solar photovoltaic applications [21,71–73].

Table 1 shows the efficiencies of various TPV diodes regarding to the References [30] and [36]. It is seen that for different temperatures, the efficiency behavior of TPV cells differs. In Table 2, the efficiency behavior of various TPV systems is shown. It is easy to see in Table 2 that the total efficiency of a system does not depend only on TPV diode efficiency, but also it depends on the burner fuel type, the emitter material, the emitter type, the emitter surface temperature, and the filter utilized.

Fig. 8. Contribution to the internal quantum efficiency, η_Q, of the top p region, J'_{qn}, the depletion region, J'_d, and the bottom n region, J'_{qp} of an illuminated p–n junction for normal incident intensity [39].
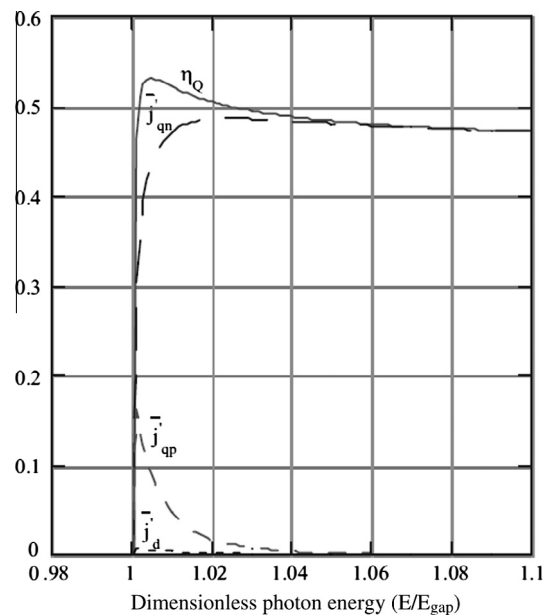
Fig. 9. Effect of recombination on the internal quantum efficiency, η_Q, of an illuminated p–n junction for normal incident intensity. Contributions from the top p region, J'_{qn}, the depletion region, J'_d, and the bottom n region, J'_{qp} [39].
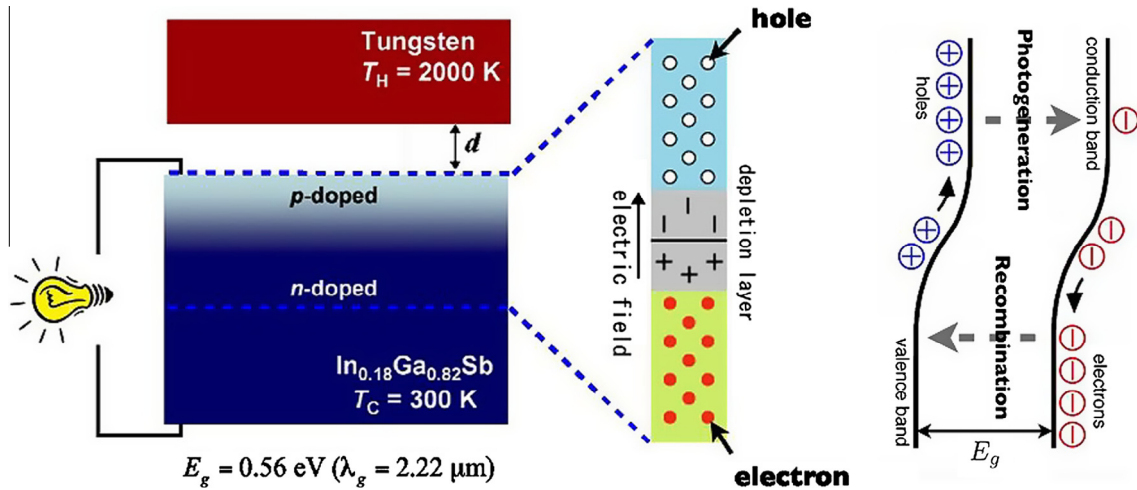
Fig. 10. Schematic of a near field TPV system with *p–n* junction, photogeneration and recombination illustration [65].
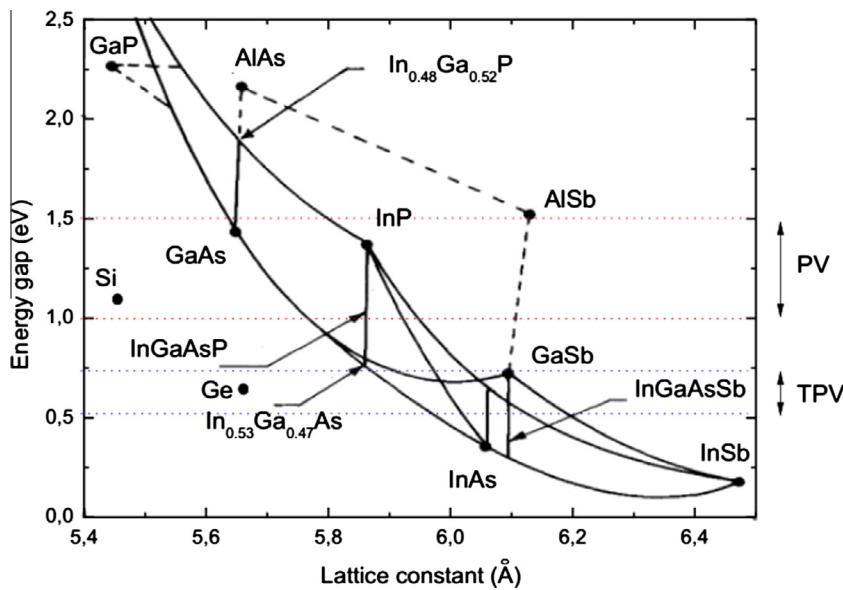
Fig. 11. Lattice constant vs. Energy gap of several TPV and PV semiconductors where the lattice matched materials are shown with perpendicular lines [21,62].
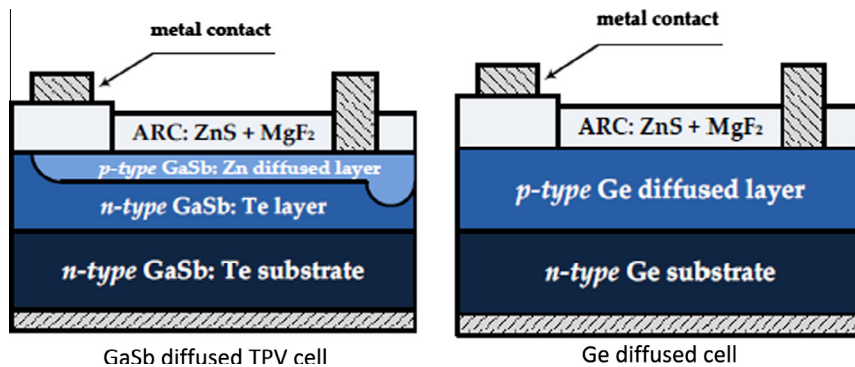
Fig. 12. Scheme of TPV cells [21].

3. The Turkish industrial sector

Turkish Industrial sector includes iron–steel, chemical–petrochemical, petrochemical–feedstock, cement, fertilizer, sugar, and non-iron metal industry and other industry. In this sector, all activities are produced by using heat energy and electricity.

Heating processes for each industry are grouped into low-, medium-, and high-temperature categories, and energy and exergy
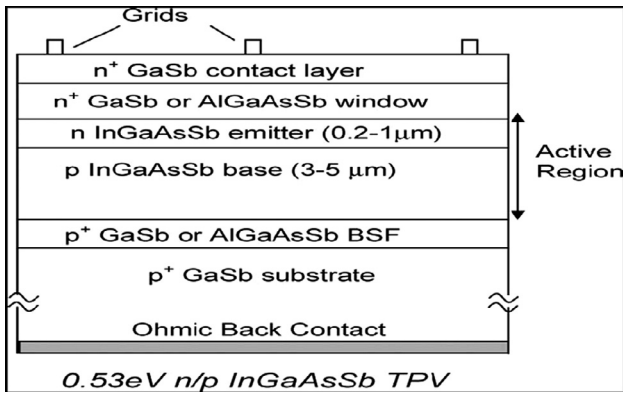
Fig. 13. Typical InGaAsSb diode [36].

Table 1
TPV efficiencies according to references.

Blackbody temperature (°C)	InGaAsSb (η_{tpv}) (%) [23]	GaSb (η_{tpv}) (%) [17]	GaAs/Ge (η_{tpv}) (%) [23]
926.85		5.9	4
950	16.9	6	4.1
1126.85		10.4	5.9
1326.85		15	8.3
1526.85		18.8	10
1726.85		21.3	10.9
1926.85		22.2	11.1
2126.85		23	11.1
2326.85		24.9	11.1

inputs to the Turkish industrial sector during 2010, as shown in Tables 3 and 4. The temperature ranges given in this table are based on the work of Brown [74], Reistad [75] and Ayres et al. [76]. The efficiencies for the low-, medium-, and high-temperature categories are obtained from Utlu and Hepbasli [1]. All mechanical drives are assumed to be 90% energy efficient.

The quality factor "q," for some energy carriers and forms has been listed elsewhere [75]. Quality of heat is Carnot factor that strongly depends on temperature, as stated in the following equation:

$$Q_{Carnot} = 1 - (T_0/T_p) \tag{10}$$

Here, T_o and T_p refer to environment and product temperatures, respectively, in the system.

Energy efficiency is a simple comparison of energy content of input and output energy carrier or flow. However, energy efficiency is defined as a function of required temperatures in the system considered.

3.1. Iron and steel industry

This subsector is a major energy consumer in the industrialized countries. Although it may show some deviations depending on these countries, in any industrialized nation, iron and steel industry accounts for 15–20% of the total industrial energy consumption and 5–10% of the total primary energy consumption. In a typical iron and steel facility, major energy inputs include coal. Electricity, natural gas, and fuel oil, heating options specified for heating systems are electrical and fuel heating. Process heating data and energy efficiency data for all categories of product heat temperature in the iron and steel sector are stated in Table 3. Also, energy consumption values are shown in Table 5 according to energy carriers. Energy efficiencies of each heating categories considered for all system efficiencies are determined, and heating system and energy preference of process are determined according to their utilization ratios.

3.2. Chemical–petrochemical industry

Steam, electricity, and by-products of some plants meet the required energy for the processes. Steam is the most important one having the biggest share, since it not only supplies energy but also involves in many process. Various energy carriers such as natural gas, fuel oil, and LPG are utilized in producing steam, which is mostly required under two different conditions. These are called low heating (47 °C) and medium heating (141 °C) as illustrated in Table 3. However, energy consumption values are shown in Table 5 according to energy carriers. Electricity is used to obtain especially for electrolysis of salt and mechanical drive.

3.3. Petrochemical–feedstock industry

Steam and by-products of some plants meet the required energy for the processes. Steam is the most important one and has the biggest share, since it supplies energy and is involved in many

Table 2
TPV system prototype efficiencies [21].

Burner fuel	Emitter material	Emitter type	Emitter surface temp. (K)	Filter	PV cells	Efficiency (%)	P_{fuel} (W)	P_{el} (W)	Type of result
	SiC	Porous foam	1558	Coatings of SiO_2 and TiO_3 on glass	GaSb		8260	123	Experi.
	Yb_2O_3 coated on Al_2O_3	Foam ceramic			Si		2000	14	Experi.
Methane	W-coated on SiC			Glass tube	GaSb		1800	30	Experi.
Methane	Kanthal				GaSb		1460	60	Experi.
	(1) Yb_2O_3 fiber felt; (2) ceramic fiber-coated on SiC	Two emitters arranged in tandem			Si GaSb	36.0 / 20.0	1920	60	Experi.
Butane	Yb_2O_3	Spherical emitter			Si		1350	15	Experi.
Butane	Yb_2O_3			Glass	Si	21.0	1985	55	Pre.
Regenerative burner	Yb_2O_3 coated on Al_2O_3			Dielectric filters	GaSb		606	66	Experi.
	Yb_2O_3				Si		2500	190	Experi.
Propane	Yb_2O_3		2100	Dielectric filters	Si		1830	165	Pre.
Butane gas	Yb_2O_3	Fibrous mantle		No	Si	10.4	305	0.11	Experi.
Methane	Yb_2O_3		1800	Quartz tube	Si	16.0	1200	120	Experi.
Hydrogen	SiC		1265	No	GaInAsSb		130	1.2	Pre.
Butane	Yb_2O_3	Porous foam	1735	SnO2 film on quartz	Si		1980	48	Experi.
Diesel	ErAG-coated on SiC		1523	Quartz tube	AlGaAs/ GaAs		1215	2976	Pre.

Table 3
Process heating data and energy efficiency data for all categories of product temperature (T_p) in the industrial sector. *Source:* [1,28,29].

Industry	Breakdown of energy used each, T_p (%)			Breakdown of energy efficiencies for each T_p category. by type		
	T_p range	Mean, T_p (°C)	Electricity (%)	Fuel (%)	$\eta_{e \cdot h}$ (%)	$\eta_{f \cdot h}$ (%)
Iron and steel	Low	45	4.2	0	100.00	65.00
	Medium	0	0	0	90.00	60.00
	High	983	95.8	100	70.00	50.00
Chemical and petrochemical	Low	42	62.5	0	100.00	65.00
	Medium	141	37.5	100	90.00	60.00
	High	494	0	0	70.00	50.00
Petrochemical–feedstock	Low	57	0	0	100.00	65.00
	Medium	227	0	0	90.00	60.00
	High	494	0	100	70.00	50.00
Fertilizer	Low	57	10	30	100.00	65.00
	Medium	350	80	30	90.00	60.00
	High	900	10	40	70.00	50.00
Cement	Low	42	91.7	0.9	100.00	65.00
	Medium	141	0	9	90.00	60.00
	High	586	8.3	90.1	70.00	50.00
Sugar	Low	83	100	59	100.00	65.00
	Medium	315	0	9	90.00	60.00
	High	400	0	32	70.00	50.00
Non-iron metals	Low	61	10	13.8	100.00	65.00
	Medium	132	9.4	22.6	90.00	60.00
	High	401	80.4	63.6	70.00	50.00
Other industry	Low	57	10.6	13.8	100.00	65.00
	Medium	132	89.4	86.2	90.00	60.00
	High	400	0.1	0.1	70.00	50.00

Table 4
Energy inputs to the Turkish industrial sector during 2010.

Energy carrier	Toe[a]		Total input		Industrial sector inputs to sector	
			(PJ)	(%)	(PJ)	(%)
Hard coal	0.61	Energy	651.93	14.36	129.78	10.76
Lignite	0.21	Energy	607.78	13.39	68.07	5.64
Asphaltite	1.03	Energy	18.80	0.41	1.76	0.15
Petroleum	1.05	Energy	1244.68	27.42	160.24	13.28
Natural gas	0.91	Energy	1450.35	31.96	297.91	24.70
Wood	0.30	Energy	142.15	3.13	0	0
Biomass	0.23	Energy	47.69	1.05	0	0
Hydro-power	0.09	Energy	186.19	4.11	288.68	23.93
Geothermal (electric)	0.86	Energy	24.013	0.53	0	0
Geothermal (heat)	1.00	Energy	58.14	1.28	51.04	4.23
Solar	1.00	Energy	18.06	0.40	5.43	0.45
Wind	0.09	Energy	10.48	0.23	0	0
Coke	0.7	Energy	73.13	1.61	73.13	6.06
Petrocoke	0.77	Energy	5.24	0.12	130.29	10.80
Total		Energy	**4538.64**	100	**1206.34**	100

[a] The values are conversion factor to tons oil of equivalent (toe).

processes. Steam is mostly required under one condition, namely high heating, as stated in Table 3. Also, energy consumption values are mentioned in Table 5 according to energy carriers.

3.4. Fertilizer industry

Natural gas is the raw material and energy supplier for the fertilizer plants as well as ammonia. Steam and electricity are the other energy inputs. Other fertilizer plants normally use electricity for drives, compressors, and cooling. In case of additional energy requirement, low quality steam is generally utilized. Utilization categories of electricity and fuel energy are presented in Table 3. Also, energy consumption values are shown in Table 5 according to energy carriers.

3.5. Cement industry

The energy used in producing cement can be divided into two parts, namely electrical energy and thermal energy. Coal, lignite, fuel oil, or natural gas are used, as thermal energy resources, in order to require low, medium, and high temperatures in the production of cement. Electricity is basically used to obtain mechanical drive at low and high temperatures in process. Also, energy consumption values are presented in Table 5 according to energy carriers.

3.6. Sugar industry

In this industry, energy utilization is required by means of electricity and fuel energy at low heating options, as indicated in

Table 5
Energy inputs to the Turkish industrial sector and its subsectors during 2010.

	TOE	Industrial total		Iron–steel		Chemical–petrochemical		Feedstock–petrochemical		Fertilizer		Cement		Sugar		Non-metal industry		Other industrial	
		Energy (PJ)	%	Energy (PJ)	%	Energy (PJ)	%	Energy (PJ)	%	Energy (PJ)	%	Energy (PJ)	%	Energy (PJ)	%	Energy (PJ)	%	Energy (PJ)	%
Hard coal	0.61	129.78	10.76	38.96	13.69	2.14	3.61	0.00	0.00	0.05	1.50	77.18	45.68	1.89	26.34	0.00	0.00	9.56	1.66
Lignite	0.21	68.06	5.64	1.18	0.41	4.28	7.22	0.00	0.00	0.00	0.00	14.12	8.36	0.82	11.39	1.77	5.61	45.88	7.97
Asphaltite	0.43	1.76	0.15	0.00	0.00	0.00	0.00	0.00	0.00	0.00	0.00	0.00	0.00	0.00	0.00	0.00	0.00	1.76	0.31
Petroleum	1.05	160.24	13.28	15.10	5.30	26.51	44.69	75.58	100.00	0.18	5.15	1.14	0.68	0.40	5.51	0.13	0.42	41.17	7.15
Natural Gas	0.91	297.91	24.70	28.19	9.90	6.31	10.64	0.00	0.00	2.66	78.07	0.61	0.36	2.13	29.73	21.19	66.98	236.82	41.15
Hydro-power	0.09	288.68	23.93	65.29	22.93	20.07	33.83	0.00	0.00	0.52	15.28	19.15	11.33	1.18	16.41	8.28	26.17	174.21	30.27
Geothermal (heat)	1.00	51.04	4.23	6.94	2.44	0.00	0.00	0.00	0.00	0.00	0.00	0.00	0.00	0.00	0.00	0.00	0.00	44.10	7.66
Solar	1.00	5.43	0.45	0.00	0.00	0.00	0.00	0.00	0.00	0.00	0.00	0.00	0.00	0.00	0.00	0.00	0.00	5.43	0.94
Petrocoke	0.63	73.13	6.06	0.00	0.00	0.00	0.00	0.00	0.00	0.00	0.00	56.78	33.60	0.00	0.00	0.26	0.83	16.09	2.80
Coke	0.70	130.29	10.80	129.04	45.33	0.00	0.00	0.00	0.00	0.00	0.00	0.00	0.00	0.76	10.62	0.00	0.00	0.47	0.08
Total		1206.34	100.00	284.68	100.00	59.32	100.00	75.58	100.00	3.41	100.00	168.98	100.00	7.16	100.00	31.63	100.00	575.50	100.00

Z. Utlu, U. Parali / Energy Conversion and Management 74 (2013) 308–322   317

Table 3. Also, energy consumption values are mentioned in Table 5 according to energy carriers.

3.7. Non-iron metal industry

This industry consists of other metals such as manufacturing of fabricated metal products. Especially, electricity and fuel are used extensively in order to obtain high temperatures for product in this sector. Also, energy consumption values are shown in Table 5 according to energy carriers.

3.8. Other industries

Others industry includes textile and yarn, glass and glassware production, paper, beverage and cigarette, food, wood, leather etc. Especially, electricity and fuel are extensively used for medium categories of product heat temperatures. Also, energy consumption values are stated in Table 5 according to energy carriers.

4. An application of the Turkish industrial sector

4.1. Usage of energy in the Turkish industrial sector

The application presented here analyzes the heat and electrical energy utilization of the TIS based on variations of dead state temperature (25 °C) of process. In the analysis, the actual data for 2010 obtained from various sources were used [1,77,78].

The structures of Turkey's total, industrial sector, and its subsectors as well as energy inputs for 2010 are listed in Table 4 and Table 5. As can be seen in these tables, total energy inputs to the whole of Turkey and TIS were 4538.64 PJ and 1206 PJ in 2010, respectively. 26.76% of total energy input was produced in 2010, while the rest has met by imports. In 2010, consumption of 13 energy sources had the biggest share of the natural gas with 31.96% followed by petroleum with 27.42%. Share of the other sources in the energy consumption is indicated in Table 4. In 2010, renewable energy source production was the second biggest production source after total coal production, providing about 42% of the energy production.

In 2010, 42% of Turkey's total end-use energy was consumed by the industrial sector. This is followed by the residential–commercial sector with 31%, the transportation sector with 19%, the agricultural sector at 4.8%, and the non-energy (out of energy) use with 3.2%.

The industrial sector of Turkey is composed of many industries, but the eight most significant industries are identified as iron–steel, chemical–petrochemical, petrochemical–feedstock, cement, fertilizer, sugar, non-iron metal industry, and other industries. In order to simplify the analysis of energy efficiencies for this complex sector, energy consumption patterns are analyzed, and the eight most significant industries (in which the total energy consumption accounts for more than 95% of the total energy used in this sector) are chosen to represent the entire sector.

In the Turkish industrial sector, the energy used to generate heat for production processes accounts for 82% of the total energy consumption, with mechanical drives, lighting, and air-conditioning accounting for 18%. In the present study, it is decided to analyze the heating and mechanical end uses only. This simplification is considered valid since heating and mechanical processes account for 95% of the energy consumption in the industrial sector, see Table 6.

Heating processes for each industry are grouped into low-, medium-, and high-temperature categories as shown in Table 3. Three steps are used to derive the overall efficiency of the sector as stated above. In the determination of sector efficiencies, weighted mean overall energy efficiencies for the major industries in the industrial sector are obtained, using the weighting factor as

Table 6
Potential of electrical production by means of TPV from waste high heating energy in the Turkish Industrial Sector.

Industry	T_p range	Mean T_p (°C)	Electricity (%)	Fuel (%)	Electric use (PJ)	Fuel use (PJ)	$\eta_{e \cdot h}$ (%)	$\eta_{f \cdot h}$ (%)	Waste energy (electricity) (PJ)	Waste energy (fuel) (PJ)	Total waste high heating (PJ)	Total waste energy (PJ)	TPV efficiencies (η_{tpv}) 5%	10%	15%
Iron and steel	Low	45	4.2	0	2.74		100	65	0	0					
	Medium	0	0	0			90	60	0	0					
	High	983	95.8	100	62.55	219.4	70	50	18.77	109.7	128.46	128.46	6.43	12.85	19.27
Chemical and petrochemical	Low	42	62.5	0	12.54		100	65	0	0					
	Medium	141	37.5	100	7.52	39.25	90	60	0.76	15.7		16.45	0.82	1.65	2.47
	High	494	0	0			70	50	0	0	0	0	0	0	0
Petrochemical–feedstock	Low	57	0	0			100	65	0	0					
	Medium	227	0	0			90	60	0	0					
	High	494	0	100		75.58	70	50	0	37.79	37.79	37.79	1.89	3.78	5.67
Fertilizer	Low	57	10	30	0.06	0.89	100	65	0	0.3115					
	Medium	350	80	30	0.42	0.9	90	60	0.042	0.36					
	High	900	10	40	0.06	1.1	70	50	0.018	0.55	0.568	0.57	0.028	0.057	0.085
Cement	Low	42	91.7	0.9	18.16	2.09	100	65	0	0.7315					
	Medium	141	0	9		13.41	90	60	0	5.364					
	High	586	8.3	90.1	1.7	134.33	70	50	0.51	67.165	67.68	67.68	3.384	6.768	10.15
Sugar	Low	83	100	59	1.18	3.47	100	65	0	1.2145					
	Medium	315	0	9		0.53	90	60	0	0.212					
	High	400	0	32		1.88	70	50	0	0.94	0.94	0.94	0.047	0.094	0.141
Non-iron metals	Low	61	10	13.8	0.83	2.336	100	65	0	0.8176					
	Medium	132	9.4	22.6	0.78	5.28	90	60	0.078	2.1117					
	High	401	80.4	63.6	6.66	14.86	70	50	1.99	7.4285	9.43	9.43	0.478	0.945	1.414
Other industry	Low	57	10.6	13.8	18.46	55.378	100	65	0	19.382					
	Medium	132	89.4	86.2	150.16	345.92	90	60	15.02	138.36					
	High	400	0.1	0.1	1.74	4.01	70	50	0.522	2.005	2.527	2.53	0.126	0.253	0.379
General total					285.55	920.61					**247.39**	447.85	22.39	44.79	67.18

the fraction of the total industrial energy demand supplied to each industry. The efficiency calculations for a non-iron metal industry are shown in detail below.

4.2. Process heat efficiency calculations for the product heat temperature categories in each industry

Product heat data and energy equations for each industry are separated into the categories defined in Table 3. The resulting breakdown is shown in Table 3, with the percentage of efficiencies in each industry supplied by electricity and fossil fuels.

4.2.1. Electrical process heat calculations

In the industrial subsectors, electrical heating is used to supply low, medium, and higher heating categories as indicated in Table 3.

The energy efficiency for this electrical end use is as follows:

$$\eta_{e \cdot h} = Q_p / W_e = 1 \tag{11}$$

Here, "$\eta_{e \cdot h}$," "Q_p," and "W_e" refer to efficiency of electrical heating, product heat, and electrical work, respectively.

4.2.2. Fossil fuel process heat calculations

The industrial subsectors require fossil fuel heating at all ranges of temperatures as given in Table 3. The energy efficiency for the low-temperature heating process is found to be 0.65 (or 65%) using the following equation:

$$\eta_{f \cdot h} = Q_p / m_f H_f \tag{12}$$

Here, "$\eta_{f \cdot h}$," "m_f," and "H_f" refer to efficiency of fuel heating, mass of fuel, enthalpy of fuel, respectively.

Similarly, the energy efficiency for the medium-temperature and high-temperature heating process is found to be equal to 60% and 50%, respectively.

4.3. Mean process heating efficiencies for all temperature categories in each industry of the industrial sector

Prior to obtaining the overall energy efficiencies for the industrial sector, the overall heating efficiencies for each industry are evaluated. The methodology is illustrated in detail for the cement industry.

4.3.1. Mean heating energy and exergy efficiencies

A combined efficiency for the three temperature categories for electric and fossil fuel processes must be calculated in order to obtain an average for overall heating in a given industry.

Numerical values are given Tables 3 and 4, and the energy efficiency for electrical heating ($\eta_{e \cdot h}$) can be evaluated as follows:

$$\eta_{e \cdot h} = \text{(Fraction in category)} \times \text{(Energy efficiency)} \tag{13}$$

$$\eta_{e \cdot h} = (10 \times 100) + (9.4 \times 90) + (80.4 \times 70)$$

$$\eta_{e \cdot h} = 74.74\%$$

Fossil fuel heating in the non-iron metal industry is used in all temperature categories. Numerical values are given Tables 3 and 4, and the energy efficiencies for fuel heating for the year 2010 are found as follows:

$$H_{f \cdot h} = (13.8 \times 65) + (22.6 \times 60) + (63.6 \times 50)$$

$$\eta_{f \cdot h} = 51.04\%$$

The fraction of total energy utilized by the non-iron metal industry for electrical (E_e) and fossil fuel (E_f) is determined for the year 2010 as follows:

For electrical energy:

$$E_e = \frac{\text{Electrical energy}}{\text{Total energy}} \tag{14}$$

$$E_e = \frac{1.83}{29.20 + 1.83} = 0.05921 \text{ (or 5.9\%)}$$

For fossil fuel energy:

$$E_f = 1.00 - 0.059 = 0.9471 \text{ (or 94.10\%)}$$

Using the calculated energy efficiencies, $\eta_{e \cdot h}$ and $\eta_{f \cdot h}$, and the fraction of electrical (E_e) and fossil fuel energy (E_f) used by the non-iron metal industry, the overall mean energy efficiencies (η_h) for heating can be calculated as follows:

$$\eta_h = [(5.9 \times 74.74) + (94.10 \times 51.04)]/(5.9 + 94.1)$$

$$\eta_h = 52.43\%$$

Following the same methodology, mean heating energy efficiencies for the other seven industries considered are determined, as stated in Table 3.

4.3.2. Overall efficiencies for the industrial sector

Overall energy ($\eta_{o \cdot h}$) efficiency of the industrial sector is calculated using equations:

$$\eta_{o \cdot h} = [(a_{1s} * \eta_{h1s}) + (a_{pc} * \eta_{hpc}) + (a_c * \eta_{hc}) + \cdots + (a_{o1} * \eta_{ho1})]/E_i \tag{15}$$

Substituting the relevant numerical values into Eq. (15), we obtained $\eta_{o \cdot h}$ = 65.73% in 2010 for overall industrial sector.

5. Result and discussion

Three principle locations of heat recovery have been identified, namely product, flue gas, and wall heat recovery. Traditional heat recovery techniques are mostly limited to flue gas heat recovery and have high capital costs. Energy flow diagram of the thermo-photovoltaic system use in the industrial sector is shown Fig. 14.

In the TIS, the total technical–potential energy recovery in the high-temperature industry using deployed and demonstrated heat recovery devices for product, flue gas, and wall heat recovery was estimated as 447.8 PJ/year. However, an estimation from 22.40 PJ/year to 67.45 PJ/year can be achieved according to the TPV efficiencies. The major reasons for the differences between technical potential and implemented saving were doubts over the cost effectiveness and the difficulty of utilization of waste heat. Electricity generation from this waste heat using TPV does not only improve the process energy efficiency, but also act as an independent power supply, since many high-temperature processes are susceptible to power failures and therefore require a backup power source. However, electricity generation from waste heat is usually considered only if no other use for the heat can be found. This makes TPV somewhat susceptible to process changes (e.g., combustion air preheating) or improvements (e.g., in refractory durability). In the following section product, flue gas and wall heat recovery are discussed using one example process to estimate energy savings.

5.1. Product heat recovery on a continuous curved caster

Most high-temperature industries considered have a product leaving the process at temperatures between 400 °C and 983 °C by cooling the product from a higher temperature to 1256 K enthalpy will be available from the hot product as shown in Fig. 15 [2]. This enthalpy could be converted to electricity by a TPV heat recovery system. Often the surplus enthalpy is accessible only
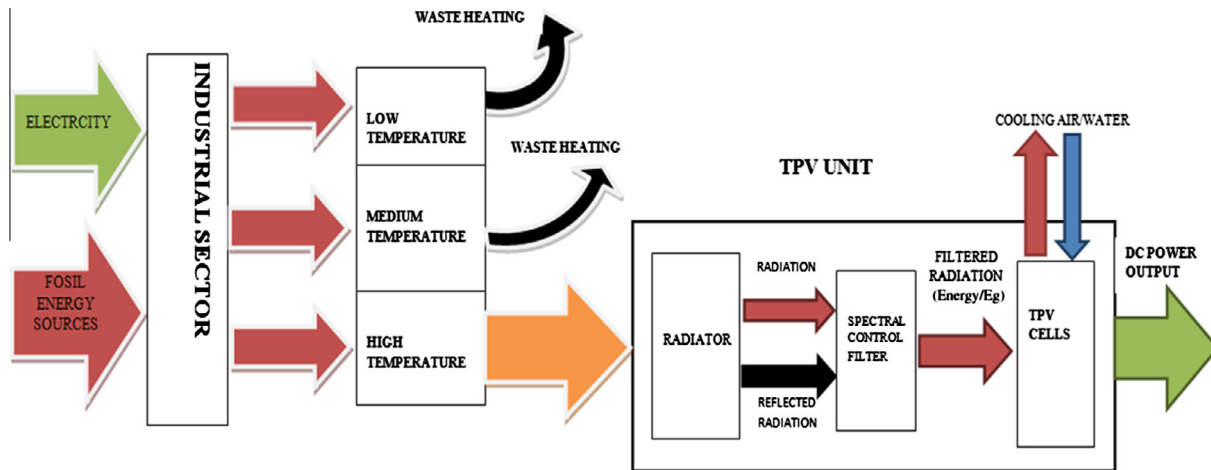
Fig. 14. Energy flow diagram of the thermophotovoltaic system use in the industrial sector.

partly, or not at all. For reasons which can include the use of other heat recovery methods (e.g., clinker cooler for air preheating), other following processes operating at high product temperature (e.g., forming of container glass) or discontinuously operating processes (e.g., slag from a blast furnace).

A continuous curved caster is discussed as an example process. Over recent decades, continuous casting methods have largely replaced the casting of ingots with subsequent reheating in soaking pits and rolling. The most common type of continuous casting machine is curved in shape and forms billets, blooms, and slabs [2]. Assuming an enthalpy of the liquid steel of 1.4 MJ/kg [79], a minimum TPV operation temperature of 1023 °C and the data in Fig. 14, it is estimated that energy of about 0.7 MJ per kg steel (11 PJ/year) for continuous casting in the TIS is in principle available for TPV conversion. There may be three locations with suitable steel temperature for TPV operation. These are the water-cooled copper mold to form a solid skin of the strand, the support area, and the guide area. In the support area, the strand with its solidified skin and liquid core is supported by rollers and cooled by water sprayers. The support area can vary over a wide range and may not be required at all (e.g., for billets with low casting speed) or extend over the full length of the machine (e.g., for a slab caster). The guide area uses less support and cooling than the support area. It is thought that the low temperature of the hot face of the copper molds around 250 °C [74,79] precludes the use of TPV in these

molds. A role for TPV is seen in the replacement of water sprayers where limitations may arise due to closed arrangement of rollers and where quality changes could occur due to fluctuations in the heat transfer rate in the cooling process. The steel-surface heat transfer rate and temperature vary along the curved caster depending on the parameters such as product cross-section, casting speed, mold system, and support system.

5.2. Flue gas heat recovery on a regenerative

In the TIS, the emitted flue gas energy from high-temperature processes is estimated as 247.39PJ/year, of which 160 PJ/year for waste gas is above 400 °C (for a total consumption of 525 PJ/year Table 3). Most high-temperature processes considered to have flue gas temperatures above 1027 °C and typically already use heat recovery methods for combustion air or product preheating, but still reject flue gases at relatively high temperatures (65 PJ/year above 400 °C). It is thought that TPV flue gas heat recovery would typically operate in a cascaded manner, where the TPV system would make use of the "high quality" heat from the actual flue gas temperature down to 1027 °C, and other heat recovery methods would utilize the remaining heat. Operation of heat exchangers has proved to be difficult partly due to flue gas contamination. Similar problems could also occur for TPV operation. Processes with flue gas cleaning at low temperature or with strict NO legislation may increase the potential of TPV [7].

5.3. Wall heat recovery on a 3-phase alternating current electric arc furnace

In the TIS, the total technical potential energy savings in the high-temperature industry for improved insulation have been estimated around 5 PJ/year, which is a relatively low value if compared with other measures such as improved combustion processes (25 PJ/year), process development (40 PJ/year), furnace and kiln design (33 PJ/year), and heat recovery (49.5 PJ/year) [2]. None of the energy losses through walls was available for this work. It is assumed here that at least 10% of the total energy consumption of high-temperature processes (Table 4. 247 PJ/ year) is lost through walls which accounts for about 27 PJ. This shows that even if the total technical potential energy saving methods are applied, there is still a large amount of energy lost (44 PJ/year). Direct energy conversion devices namely thermoelectrics and TPV are advantageous technologies for wall heat recovery, because of their modularity and the direct use of the wall heat flux without any further
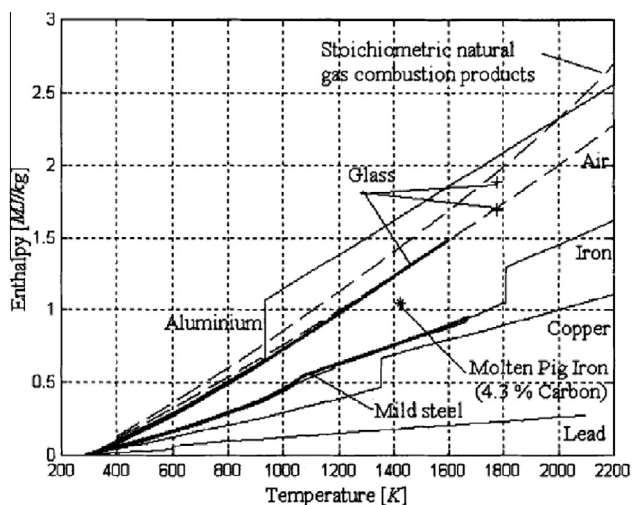

Fig. 15. Examples of heat stored in products and flue gas ducts and flue gas [2].

intermediary energy conversion into work. Typically, a high-temperature wall consists of a refractory layer at the hot side to withstand the process chamber environment and one or more insulation layers on the outer surface. If insulation thickness is increased, the temperature of the refractory layer will increase resulting in enhanced refractory consumption. This mechanism and the insulation cost are the major limiting factors for improved insulation. Heat transfer in refractories is usually complex, since refractories are often of porous or fibrous type where not only conduction but also radiation and convection heat transfer occur [2]. A 3-phase alternating current electric arc furnace (EAF) is discussed as an example process. EAFs are cylindrical refractory lined vessels with usually three carbon electrodes that can be raised or lowered through a removable furnace roof. They are used to produce carbon and alloy steels in a batch process. Cycles range from about 1.5 to 5 h to produce carbon steel and from 5 to 10 h or more to produce alloy steel. The feedstock is mainly scrap steel and waste pig iron from steel works. Power is supplied mainly by electricity using a 3-phase alternating current which creates arcs between the electrodes that melt the metallic charge. Additionally, oxygen-fuel burners are widely employed to assist melting. Water-cooling for the roof and sidewall panels of EAF furnaces is becoming common practice. In principle, these panels could be replaced by a TPV heat recovery system where the available water supply could be used for PV cell cooling. A case study, utilizing the data of a typical 80 tonne furnace [2], for TPV efficiency of 20% and power density of $1.0 \, \text{W/cm}^2$ suggests that about 4% of the total energy input (0.65 PJ/year in the TIS) could be recovery as electricity by using TPV in the roof and sidewalls. Other potential processes are the metallurgical reactor for secondary refining in the steel industry the conditioning zone of glass furnaces (especially float glass) and water-cooled areas in the blast furnace.

6. Conclusions

This study has investigated the potential of TPV heat recovery systems for the improvement of energy efficiency for the high-temperature district of the TIS based on actual data of Turkey for 2010. Ordinary solar PV is liable to various changing operation conditions including the angle of the solar radiation, the cell temperature, and the radiation spectrum. In contrast, TPV operates under more constant conditions and has the possibility to recover radiation by spectral control.

- Both of these factors allow higher efficiency for TPV. In addition, TPV has a greater power density (about 100 times) and a longer operation time in industrial processes (up to 24 h a day) as compared to PV; these characteristics should keep payback periods short.
- Direct energy conversion devices can be used in all locations, while thermoelectrics could recover waste heat for low-temperature processes (<127 °C), and TPV can be used the high-temperature processes heat (>1027 °C).
- Advances in both technologies may allow the entire temperature range to be covered using direct energy conversion devices.
- An overall assessment of TPV in the high-temperature industry is complex, mainly because of the large process diversity and causes an individual evaluation for each process where TPV usage is required.
- In the TIS, the total technical–potential energy recovery in the high-temperature industry using deployed and demonstrated heat recovery devices for product, flue gas, and wall heat recovery was estimated as 447.8 PJ/year. However, an estimation from 22.40 PJ/year to 67.45 PJ/year can be achieved according to the TPV efficiencies.

- The example processes may allow the generation of electricity of several PJ/year, so resulting in CO_x savings of several 100,000 tonnes annually (using a conversion factor of 122.2 kgCO_x/GJ for TIS electricity generation). This suggests that there is a large potential of electricity generation in the industry using TPV, which could improve industrial energy efficiency and could act as a backup power supply for power failures.
- Future work requires the demonstration of TPV technology in these locations for a range of radiator temperatures associated with different power densities.
- Potential of TPV of the industrial sector was compared for the eight subsectors for 2010. The iron and steel subsectors have the most technical potential due to their proper match of high-temperature application with high quality energy resources.
- It may be concluded that the analysis reported here will provide the investigators with a better quantitative grasp of the inefficiencies and their relative magnitudes in evaluating the energy utilization performance as well as in developing energy policies of countries.

References

[1] Utlu Z, Hepbasli A. Parametrical investigation of the effect of dead (reference) state on energy and exergy utilization efficiencies of residential–commercial sectors: a review and an application. Renew Sustain Energy Rev 2007;11(4):603–34.

[2] Bauer T, Forbes I, Pearsall N. The potential of thermophotovoltaic heat recovery for the UK industry. Int J Ambient Energy 2004;25(1):19–25.

[3] Coutts TJ. A review of progress in thermophotovoltaic generation of electricity, National Renewable Energy Laboratory, USA. Renew Sustain Energy Rev 1999;3:77–184.

[4] Fraas L, Avery J, Daniels W, Huang HX, Malfa E. TPV tube generators for apartment building and industrial furnace applications. In: 17th European photovoltaic solar energy conference; 2001.

[5] Fraas LM, Avery JE, Daniels WE, Huang HX, Malfa E, Venturino M, et al. TPV tube generators for apartment building and industrial furnace applications in thermophotovoltaic generation of electricity. In: Fifth conference on thermophotovoltaics. Rome: American Institute of Physics; 2003. ISBN:0735401 136.

[6] Glass Project Fact Sheet – Thermophotovoltaic electric power generation using exhaust heat. U.S. Department of Energy, Office of Industrial Technologies; 2001.

[7] Bauer T, Forbes I, Penlington R, Pearsall N. The potential of thermophotovoltaic heat recovery for the glass industry in thermophotovoltaic generation of electricity. In: Fifth conference on thermophotovoltaic. Rome: American Institute of Physics; 2003. ISBN:0735401 136.

[8] Colangelo A, de Risi A, Laforgia A. Experimental study of a burner with high temperature heat recovery system for TPV applications. Energy Convers Manage 2006;47:1192–206.

[9] Hugues LT, Beyene A. Heat recovery from automotive engine. Appl Therm Eng 2009;29:439–44.

[10] Larjola J. Electricity from lndustrial waste heat using high-speed organic Rankine Cycle. Int J Prod Econ 1995;41:227–35.

[11] Law R et al. Opportunities for low-grade heat recovery in the UK food processing industry. Appl Therm Eng 2012. http://dx.doi.org/10.1016/j.applthermaleng.2012.03.024.

[12] Korobitsyn M. Industrial applications of the air bottoming cycle. Energy Convers Manage 2002;43:1311–22.

[13] Rowe DM, Min G. Evaluation of thermoelectric modules for power generation. J Power Sources 1998;73:193–8.

[14] Bouzid F, Dehimi L. Performance evaluation of a GaSb thermophotovoltaic converter. Revue des Energies Renouvelables 2012;15(3):383–97.

[15] Shinners M. Empfasis – February 2011 – advanced materials for TPV devices. <http://www.empf.org/empfasis/2011/February11/advanced.html> [accessed July 2012].

[16] Catalano A. Thermophotovoltaics: a new paradigm for power generation. Renew Energy Spec Issue World Renew Energy Cong, Energy Eff Environ 1996;8(1–4):495–9.

[17] Coutts TJ. An overview of thermophotovoltaic generation of electricity. Sol Energy Mater Sol Cells 2001;66:443–52.

[18] Yang WM, Chou SK, Shu C, Xue H, Li ZW, Li DT, et al. Microscale combustion research for application to micro thermophotovoltaics systems. Energy Convers Manage 2003;44:2625–34.

[19] Bermel P, Ghebrebrhan M, Chan W, Yeng YX, Araghchini M, Hamam R, et al. Design and global optimization of high-efficiency thermophotovoltaic systems. Opt Express 2010;18(103):A314.

[20] Fraas LM, Avery JE, Huang HX, Martinelli RU. Thermophotovoltaic system configurations and spectral control. Semicond Sci Technol 2003;18:165–73.
[21] Bosi M, Ferrari C, Melino F, Pinelli M, Spina PR, Venturini M. Thermophotovoltaic generation: a state of the art review. In: Proceedings of the 25th int conf on efficiency, cost, optimization, simulation and environmental impact of energy systems 2012, Perugia, Italy.
[22] DeBellis CL, Scoto MV, Fraas L, Samaras J, Waston RC, Scoles SW. Component development for 500 Watt diesel fueled portable thermophotovoltaic power supply. AIP Conf Proc 1999;460:362.
[23] Becker FE, Doyle FE, Shukla K. Operating experience of a portable thermophotovoltaic power supply. AIP Conf Proc 1999;460:394.
[24] Fraas L, Ballantyne R, Hui S, Ye SZ, Gregory S, Keyes J, et al. Commercial GaSb cell and circuit development for the Midnight Sun TPV stove. AIP Conf Proc 1999;460:480.
[25] Stone KW, Chubb DL, Wilt DM, Wanlass MW. Testing and modeling of a solar thermophotovoltaic power system. AIP Conf Proc 1996;460:358.
[26] Morrison O, Seal M, West E, Connely W. Use of a thermophotovoltaic generator in a hybrid electric vehicle. AIP Conf Proc 1999;460:488.
[27] Coutts T. In: Archer MD, Hill R, editors. Clean electricity from photovoltaics. Imperial College Press; 2001.
[28] Kruger JS, Guazzoni G, Nawrocki SJ. U.S. Army thermophotovoltaic effects. AIP Conf Proc 1999;460:30.
[29] www.thermalfluidscentral.org.
[30] Andreev VM, Khvostikova VP, Khvostikova OA, Rumyantsev VD, Gazarjan PY, Vlasov AS. Solar thermophotovoltaic converters: efficiency potentialities. In: Conf on thermophotovoltaic generation of electricity; 2004.
[31] Qiu K, Hayden ACS. Thermophotovoltaic generation of electricity in a gas fired heater: influence of radiant burner configurations and combustion processes. Energy Convers Manage 2003;44:2779–89.
[32] Colangelo A, de Risi A, Laforgia A. Experimental study of a burner with high temperature heat recovery system for TPV applications. Energy Convers Manage 2006;47:1192–206.
[33] Lindler KW, Harper MJ. Combuster/Emitter design tool for a thermophotovoltaic energy converter. Energy Convers Manage 1998;39:391–8.
[34] Bauer T. Thermophotovoltaics: basic principles and critical aspects of system design. Berlin: Springer; 2011. ISBN:1865-3529.
[35] Zhai X, Lai J, Liang H, Chen S. Performance analysis of thermophotovoltaic system with an equivalent cut-off blackbody emitter. J Appl Phys 2010;108:074507.
[36] Dashiell MW et al. Quaternary InGaAsSb thermophotovoltaic diodes. IEEE Trans Electron Dev 2006;53(12).
[37] Fourspring PM, DePoy DM, Rahmlow TD, Lazo-Wasem JE, Gratrix EJ. Optical coatings for thermophotovoltaic spectral control. Appl Opt 2006;45(7):1356–8.
[38] Uppal PN, Charache G, Baldasaro P, Campbell B, Loughin S, Svensson S, et al. MBE growth of GaInAsSb p/n junction diodes for thermophotovoltaic applications. J Cryst Growth 1997;175:877–82.
[39] Chubb DL. Fundamentals of thermophotovoltaic energy conversion. Amsterdam: Elsevier; 2007. ISBN:978-0-444-52721-9.
[40] Yang WM, Chou SK, Shu C, Xue H, Li ZW, Li DT, et al. Microscale combustion research for application to micro thermophotovoltaic systems. Energy Convers Manage 2003;44:2625–34.
[41] Epstein AH, Senturia SD, et al. Micro-heat engines, gas turbines, and rocket engines-the MIT Microengine project. AIAA 1997;1773:1–12.
[42] Epstein AH, Senturia SD, et al. Power MEMS and microengines. In: IEEE transducers conference, Chicago, IL; 1997. p. 753–6.
[43] Fahrenbruch AL, Bube RH. Fundamentals of solar cells: photovoltaic solar energy conversion. New York: Academic Press; 1983.
[44] Bube RH. Photovoltaic materials. London: Imperial College Press; 1998.
[45] Rahmlow TD, Lazo-Wasem JE, Gratrix EJ, Fourspring PM, Depoy DM. Design considerations and fabrication results for front surface TPV spectral control filters. In: Proc 6th conf thermophotovoltaic generation of electricity, vol. 738; 2004. p. 180–8.
[46] Hickey CF, et al. Antimony selenide in multilayer coatings. In: Optical interference coatings, OSA Technical Digest, ThE4-1/3, vol.9; 2001.
[47] Depoy DM, et al. Interference filters for thermophotovoltaic applications. Optical interference coatings, OSA Technical Digest, ThC5-1/2; 1998.
[48] Ortabasi U, Bovard B. Rugate technology for thermophotovoltaic (TPV) applications: a new approach to near perfect filter performance. In: 5th Conf of thermophotovoltaic generation of electricity. American Institute of Physics; 2003.
[49] Jarefors K, et al. Optical interference filters in thermophotovoltaic applications. Optical interference coatings, OSA Technical Digest, ThC6-1/3, vol. 9; 1998.

[50] Rahmlow, TD, Jr., Depoy DM, Fourspring PM, Ehsani H, Lazo-Wesam JE, Gratrix EJ. Development of front surface, spectral control filters with great temperature stability for thermophotovoltaic energy conversion. In: Proc of 7th conf on thermophotovoltaic generation of electricity, vol. 890; 2007. p 59–67.
[51] Nagashima T, Okumura K, Yamaguchi M. A germanium back contact type thermophotovoltaic cell. In: Proc of 7th conf. on thermophotovoltaic generation of electricity, vol. 890; 2006. p. 172–81.
[52] Mattarolo G, Bard J, Schmid J. Experimental testing and modelling approach for a TPV prototype. In: Proc of 7th conf on thermophotovoltaic generation of electricity, vol. 890; 2006. p 264–72.
[53] O'Sullivan F, Celanovic I, Jovanovic N, Kassakian J. Optical characteristics of one-dimensional Si/SiO$_2$ photonic crystals for thermophotovoltaic applications. J Appl Phys 2005;97:033529.
[54] Lee HY, Cho SJ, Nam GY. Multiple wavelength transmission filters based on Si–SiO$_2$ one dimensional photonic crystals. J Appl Phys 2005;97:103111.
[55] Joannopoulos JD, Johnson SG, Winn JN, Meade RD. Photonic crystals: molding the flow of light. 2nd ed. Princeton; 2008.
[56] Celanovic I, Perreault D, Kassakian J. Resonant cavity enhanced thermal emission. Phys Rev B 2005;72:075127.
[57] Celanovic I, Jovanovic N, Kassakian J. Two-dimensional tungsten photonic crystals as selective thermal emitters. Appl Phys Lett 2008;92:193101.
[58] John S, Wang R. Metallic photonic band gap filament architectures for optimized incandescent lighting. Phys Rev A 2008;78:043809.
[59] Toossi R. Energy and environment: resources, technologies and impacts. 2nd ed. Verve Publishers Inc.; 2005.
[60] Hudait MK, Brenner M, Ringel SA. Effect of window layer on In$_{0.69}$Ga$_{0.31}$As thermophotovoltaic devices grown on InAs$_y$P$_{1-y}$ step graded buffers by molecular beam epitaxy. Solid State Electron 2009;53:102–6.
[61] Chan W, Huang R, Wang C, Kassakian J, Joannopoulos J, Celanovi I. Modeling low band gap thermophotovoltaic diodes for high-efficiency portable power generators. Sol Energy Mater Sol Cells 2010;94:509–14.
[62] Saleh BEA, Teich MC. Fundamentals of photonics. John Wiley & Sons; 1991. ISBN:0-471-83965-5.
[63] www.pveducation.org/pvcdrom/solar-cell-operation/quantum-efficiency.
[64] http://www.eere.energy.gov/basics/renewable_energy/pv_cell_quantum_efficiency.html.
[65] http://www.thermalfluidscentral.org/encyclopedia/index.php/Near-field_thermophotovoltaics.
[66] Mauk MG. Mid-infrared semiconductor optoelectronics. Springer Ser Opt Sci 2006;118:673–738.
[67] Khvostikov VP, Khvostikova OA, Gazaryan PY, Sorokina SV, Potapovich NS, Maleskaya AV, et al. Photo converters for solar TPV systems. In: Conf record of IEEE photovoltaic energy conversion; 2006.
[68] Anikeev S, Donetski D, Belenski G, Luryi S, Wang CA, Borrego JM, et al. Measurement of the Auger recombination rate in p-type 0.54 eV GaInAsSb by time resolved photoluminescence. Appl Phys Lett 2003;83(25):4769–71.
[69] Donetski D, Anikeev S, Gu N, Belenky G, Luryi S, Wang CA, et al. Analysis of recombination processes in 05–06 eV epitaxial GaInAsSb lattice matched to GaSb. In: Proc 6th conf thermophotovoltaic generation of electricity, vol. 738; 2004. p 320–8.
[70] Sze SM. Physics of semiconductor devices. John Wiley and Sons; 1969.
[71] Bosi M, Pelosi C. The potential of III–V semiconductors as terrestrial photovoltaic devices. Prog Photovolt Res Appl 2007;15:51–68.
[72] Chan WR, et al. Toward high energy density, high efficiency and moderate temperature chip-scale thermophotovoltaics. Appl Phys Sci, PNAS Early Edition; 2012.
[73] Wr Chan et al. Modeling low band gap thermophotovoltaic diodes for high efficiency portable power generators. Sol Energy Mater Sol Cells 2010;94:509–14.
[74] Brown S. Single-site and industrial-scale schemes. Appl Energy 1996;53:149–55.
[75] Reistad GM. Available energy conversion and utilization in the United States. ASME J Eng Power 1975;97:429–34.
[76] Ayres RU, Ayres LW, Warr B. Exergy power and work in the US economy 1900–1998. Energy 2003;28:219–73.
[77] SIS. State Institute of Statistics. Statistical yearbook of Turkey in 2010. Ankara: Prime Ministry Republic of Turkey; 2012.
[78] World Energy Council (WEC) – Turkish National Committee (TNC). 2010 Energy report. Ankara, Turkey: WEC-TNC; 2012.
[79] Beer J, Worrell E, Blok K. Future technologies for energy-efficient iron and steel making. Annu Rev Energy Env 1998;23:123–205.